

# 3

## *Thermal Equilibrium*

### 3.1 Introduction

The temperature in a static nebula is fixed by the equilibrium between heating by photoionization and cooling by recombination and by radiation from the nebula. When a photon of energy  $h\nu$  is absorbed and causes an ionization of H, the photoelectron produced has an initial energy  $\frac{1}{2}mu^2 = h(\nu - \nu_0)$ , and we may think of an electron being "created" with this energy. The electrons thus produced are rapidly thermalized, as indicated in Chapter 2, and in ionization equilibrium these photoionizations are balanced by an equal number of recombinations. In each recombination, a thermal electron with energy  $\frac{1}{2}mu^2$  disappears, and an average of this quantity over all recombinations represents the mean energy that "disappears" per recombination. The difference between the mean energy of a newly created photoelectron and the mean energy of a recombining electron represents the net gain in energy by the electron gas per ionization process. In equilibrium this net energy gain is balanced by the energy lost by radiation, chiefly by electron collisional excitation of bound levels of abundant ions, followed by emission of photons that can escape from the nebula. Free-free emission, or bremsstrahlung, is another, less important radiative energy-loss mechanism.

### 3.2 Energy Input by Photoionization

Let us first examine the energy input by photoionization. As in Chapter 2, it is simplest to begin by considering a pure H nebula. At any specific point in the nebula, the energy input (per unit volume per unit time) is

$$G(\text{H}) = n(\text{H}^0) \int_{\nu_0}^{\infty} \frac{4\pi J_{\nu}}{h\nu} h(\nu - \nu_0) a_{\nu}(\text{H}^0) d\nu \text{ [erg cm}^{-3}\text{s}^{-1}\text{]}. \quad (3.1)$$

**Table 3.1**  
Mean input energy of photoelectrons

$T_*$ (K)	$T_i$ (K)			
	$\tau_0 = 0$	$\tau_0 = 1$	$\tau_0 = 5$	$\tau_0 = 10$
$3.0 \times 10^4$	$1.58 \times 10^4$	$1.87 \times 10^4$	$3.36 \times 10^4$	$5.02 \times 10^4$
$3.5 \times 10^4$	$2.08 \times 10^4$	$2.48 \times 10^4$	$4.24 \times 10^4$	$5.94 \times 10^4$
$4.0 \times 10^4$	$2.48 \times 10^4$	$3.01 \times 10^4$	$5.48 \times 10^4$	$8.15 \times 10^4$
$5.0 \times 10^4$	$3.33 \times 10^4$	$4.12 \times 10^4$	$7.50 \times 10^4$	$10.60 \times 10^4$

Furthermore, since the nebula is in ionization equilibrium, we may eliminate  $n(\text{H}^0)$  by substituting Equation (2.8), giving

$$G(\text{H}) = n_e n_p \alpha_A(\text{H}^0, T) \frac{\int_{\nu_0}^{\infty} \frac{4\pi J_\nu}{h\nu} h(\nu - \nu_0) a_\nu(\text{H}^0) d\nu}{\int_{\nu_0}^{\infty} \frac{4\pi J_\nu}{h\nu} a_\nu(\text{H}^0) d\nu} \quad (3.2)$$

$$= n_e n_p \alpha_A(\text{H}^0, T) \frac{3}{2} kT_i$$

From this equation it can be seen that the mean energy of a newly created photoelectron depends on the form of the ionizing radiation field, but not on the absolute strength of the radiation. The rate of creation of photoelectrons depends on the strength of the radiation field, or, as Equation (3.2) shows, on the recombination rate. The quantity  $\frac{3}{2}kT_i$  represents the initial temperature of the newly created photoelectrons. For assumed blackbody spectra with  $J_\nu = B_\nu(T_*)$ , it is easy to show that  $T_i \approx T_*$  so long as  $kT_* < h\nu_0$ . For any known  $J_\nu$  (for instance, the emergent spectrum from a model atmosphere), the integration can be carried out numerically; a short list of representative values of  $T_i$  is given in Table 3.1. Note that the second column in the table,  $\tau_0 = 0$ , corresponds to photoionization by the emergent model-atmosphere spectrum. At larger distances from the star, the spectrum of the ionizing radiation is modified by absorption in the nebula, the radiation nearest the series limit being most strongly attenuated because of the frequency dependence of the absorption coefficient. Therefore, the higher-energy photons penetrate further into the gas, and the mean energy of the photoelectrons produced at larger optical depths from the star is higher. This effect is shown for a pure H nebula in the columns labeled with values of  $\tau_0$ , the optical depth at the ionization limit.

**Table 3.2**  
Recombination cooling coefficient (in  $\text{cm}^3 \text{s}^{-1}$ ).

$T(\text{K})$	$\beta_A$	$\beta_1$	$\beta_B$
2,500	$9.02 \times 10^{-13}$	$3.22 \times 10^{-13}$	$5.80 \times 10^{-13}$
5,000	$5.48 \times 10^{-13}$	$2.23 \times 10^{-13}$	$3.24 \times 10^{-13}$
10,000	$3.25 \times 10^{-13}$	$1.52 \times 10^{-13}$	$1.73 \times 10^{-13}$
20,000	$1.88 \times 10^{-13}$	$1.00 \times 10^{-13}$	$8.75 \times 10^{-14}$

### 3.3 Energy Loss by Recombination

The kinetic energy lost by the electron gas (per unit volume per unit time) in recombination can be written

$$L_R(\text{H}) = n_e n_p k T \beta_A(\text{H}^0, T), \quad [\text{erg cm}^{-3} \text{s}^{-1}] \quad (3.3)$$

where

$$\beta_A(\text{H}^0, T) = \sum_{n=1}^{\infty} \beta_n(\text{H}^0, T) = \sum_{n=1}^{\infty} \sum_{L=0}^{n-1} \beta_{nL}(\text{H}^0, T) \quad [\text{cm}^3 \text{s}^{-1}] \quad (3.4)$$

with

$$\beta_{nL}(\text{H}^0, T) = \frac{1}{kT} \int_0^{\infty} u \sigma_{nL}(\text{H}^0, T) \frac{1}{2} m u^2 f(u) du. \quad (3.5)$$

The left-hand side of Equation (3.5) is thus effectively a kinetic energy averaged recombination coefficient. Note that since the recombination cross sections are approximately proportional to  $u^{-2}$ , the electrons of lower kinetic energy are preferentially captured, and the mean energy of the captured electrons is somewhat less than  $\frac{3}{2}kT$ . Calculated values of  $\beta_1$  and  $\beta_A$  are listed in Table 3.2.

In a pure H nebula that had no radiation losses, the thermal equilibrium equation would be

$$G(\text{H}) = L_R(\text{H}), \quad (3.6)$$

and the solution for the nebular temperature would give a  $T > T_i$  because of the "heating" due to the preferential capture of the slower electrons.

The radiation field  $J_\nu$  in Equation (3.1) should, of course, include the diffuse radiation as well as the stellar radiation modified by absorption. This can easily be included in the on-the-spot approximation, since, according to it, every emission of an ionizing photon during a recombination to the level  $n = 1$  is balanced by absorption of the same photon at a nearby spot in the nebula. Thus production of photons by the diffuse radiation field and recombinations to the ground level can simply be omitted from the gain and loss rates, leading to the equations

$$\begin{aligned} G_{OTS}(\text{H}) &= n(\text{H}^0) \int_{\nu_0}^{\infty} \frac{4\pi J_{\nu s}}{h\nu} h(\nu - \nu_0) a_\nu(\text{H}^0) d\nu \\ &= n_e n_p \alpha_B(\text{H}^0, T) \frac{\int_{\nu_0}^{\infty} \frac{4\pi J_{\nu s}}{h\nu} h(\nu - \nu_0) a_\nu(\text{H}^0) d\nu}{\int_{\nu_0}^{\infty} \frac{4\pi J_{\nu s}}{h\nu} a_\nu(\text{H}^0) d\nu} \end{aligned} \quad (3.7)$$

and

$$L_{OTS}(\text{H}) = n_e n_p kT \beta_B(\text{H}^0, T), \quad (3.8)$$

with

$$\beta_B(\text{H}^0, T) = \sum_{n=2}^{\infty} \beta_n(\text{H}^0, T). \quad (3.9)$$

The on-the-spot approximation is not as accurate for the thermal equilibrium as it is in the ionization equation, because of the fairly large difference in  $h(\nu - \nu_0)$  between the ionizing photons in the stellar and diffuse radiation fields, but it may be improved by further iterations if necessary.

The generalization to include He in the heating and recombination cooling rates is straightforward to write, namely,

$$G = G(\text{H}) + G(\text{He}), \quad (3.10)$$

where

$$G(\text{He}) = n_e n(\text{He}^+) \alpha_A(\text{He}^0, T) \frac{\int_{\nu_2}^{\infty} \frac{4\pi J_\nu}{h\nu} h(\nu - \nu_2) a_\nu(\text{He}^0) d\nu}{\int_{\nu_2}^{\infty} \frac{4\pi J_\nu}{h\nu} a_\nu(\text{He}^0) d\nu} \quad (3.11)$$

and

$$L_R = L_R(\text{H}) + L_R(\text{He}), \quad (3.12)$$

with

$$L_R(\text{He}) = n_e n(\text{He}^+) kT \beta_A(\text{He}^0, T) \quad (3.13)$$

and so on.

It can be seen that the heating and recombination cooling rates are proportional to the densities of the ions involved, so the contributions of the heavy elements, which are much less abundant than H and He, can, to a good approximation, be omitted from these rates.

### 3.4 Energy Loss by Free-Free Radiation

Next we will examine cooling by radiation processes that do not involve recombination. In most circumstances such cooling is far more important than the recombination cooling, and therefore dominates the thermal equilibrium. A minor contributor to the cooling rate, which nevertheless is important because it can occur even in a pure H nebula, is free-free radiation or bremsstrahlung, in which a continuous spectrum is emitted. The rate of cooling by this process by ions of charge  $Z$ , integrated over all frequencies, is, to a fair approximation,

$$\begin{aligned} L_{FF}(Z) &= 4\pi j_{ff} \\ &= \frac{2^5 \pi e^6 Z^2}{3^{3/2} h m c^3} \left( \frac{2\pi kT}{m} \right)^{1/2} g_{ff} n_e n_+ \text{ [erg cm}^{-3} \text{ s}^{-1}] \\ &= 1.42 \times 10^{-27} Z^2 T^{1/2} g_{ff} n_e n_+ \end{aligned}$$

where  $n_+$  is the number density of the ions. Again  $\text{H}^+$  dominates the free-free cooling, because of its abundance, and  $\text{He}^+$  can be included with  $\text{H}^+$  (since both have  $Z = 1$ ) by writing  $n_+ = n_p + n(\text{He}^+)$ . The numerical factor  $g_{ff}$  is called the mean Gaunt factor for free-free emission; it is a slowly varying function of  $n_e$  and  $T$ , generally for nebular conditions in the range  $1.0 < g_{ff} < 1.5$ , and a good average value to adopt is  $g_{ff} \approx 1.3$ .

### 3.5 Energy Loss by Collisionally Excited Line Radiation

A far more important source of radiative cooling is collisional excitation of low-lying energy levels of common ions, such as  $\text{O}^+$ ,  $\text{O}^{++}$ , and  $\text{N}^+$ . These ions make a significant contribution in spite of their low abundance because they have energy levels with excitation potentials of the order of  $kT$ , but all the levels of H and He have much higher excitation potentials, and therefore are usually not important as collisionally excited coolants. Let us therefore examine how an ion is excited to level 2 by electron collisions with ions in the lower level 1. The cross section for excitation

$\sigma_{12}(u)$  is a function of electron velocity  $u$  and is zero below the threshold  $\chi = h\nu_{21}$ . Not too far above the threshold, the main dependence of the excitation cross section is  $\sigma \propto u^{-2}$  (because of the focusing effect of the Coulomb force); so it is convenient to express the collision cross sections in terms of the energy-specific collision strength  $\Omega(1, 2)$  defined by

$$\sigma_{12}(u) = \frac{\pi \hbar^2}{m^2 u^2} \frac{\Omega(1, 2)}{\omega_1} \quad \text{for } \frac{1}{2} mu^2 > \chi, \quad (3.14)$$

where  $\Omega(1, 2)$  is a function of electron velocity (or energy) but is often approximately constant near the threshold, and  $\omega_1$  is the statistical weight of the lower level.

There is a relation between the cross section for deexcitation,  $\sigma_{21}(u)$ , and the cross section for excitation, namely

$$\omega_1 u_1^2 \sigma_{12}(u_1) = \omega_2 u_2^2 \sigma_{21}(u_2) \quad (3.15)$$

where  $u_1$  and  $u_2$  are related by

$$\frac{1}{2} mu_1^2 = \frac{1}{2} mu_2^2 + \chi. \quad (3.16)$$

Equation (3.15) can easily be derived from the principle of detailed balancing, which states that in thermodynamic equilibrium each microscopic process is balanced by its inverse. Thus in this particular case, the number of excitations caused by collisions with electrons in the velocity range  $u_1$  to  $u_1 + du_1$  is just balanced by the deexcitations caused by collisions that produce electrons in the same velocity range. Thus

$$n_e n_1 u_1 \sigma_{12}(u_1) f(u_1) du_1 = n_e n_2 u_2 \sigma_{21}(u_2) f(u_2) du_2,$$

and using the Boltzmann equation of thermodynamic equilibrium,

$$\frac{n_2}{n_1} = \frac{\omega_2}{\omega_1} \exp(-\chi/kT),$$

we derive the relation (3.15). Combining Equations (3.14) and (3.15), so that the deexcitation cross section can be expressed in terms of the collision strength  $\Omega(1, 2)$ ,

$$\sigma_{21}(u_2) = \frac{\pi \hbar^2}{m^2 u_2^2} \frac{\Omega(1, 2)}{\omega_2}; \quad (3.17)$$

that is, the collision strengths are symmetrical in 1 and 2.

The total collisional deexcitation rate per unit volume per unit time is

$$\begin{aligned} n_e n_2 q_{21} &= n_e n_2 \int_0^\infty u \sigma_{21} f(u) du \\ &= n_e n_2 \left( \frac{2\pi}{kT} \right)^{1/2} \frac{\hbar^2}{m^{3/2}} \frac{\Upsilon(1, 2)}{\omega_2} [\text{cm}^{-3} \text{s}^{-1}] \\ &= n_e n_2 \frac{8.629 \times 10^{-6}}{T^{1/2}} \frac{\Upsilon(1, 2)}{\omega_2} \end{aligned} \quad (3.18)$$

where  $\Upsilon(1, 2)$  is the velocity-averaged collision strength

$$\Upsilon(1, 2) = \int_0^\infty \Omega(1, 2; E) \exp(-E/kT) d \left( \frac{E}{kT} \right) \quad (3.19)$$

with  $E = \frac{1}{2} m u^2$ . Likewise, the collisional excitation rate per unit volume per unit time is  $n_e n_1 q_{12}$ , where

$$\begin{aligned} q_{12} &= \frac{\omega_2}{\omega_1} q_{21} \exp(-\chi/kT) \\ &= \frac{8.629 \times 10^{-6}}{T^{1/2}} \frac{\Upsilon(1, 2)}{\omega_1} \exp(-\chi/kT) [\text{cm}^3 \text{s}^{-1}] \end{aligned} \quad (3.20)$$

The collision strengths must be calculated quantum-mechanically, and some of the most important numerical values are listed in Tables 3.3 through 3.7. Each collision strength in general consists of a part that varies slowly with energy, on which, in many cases, there are superimposed resonance contributions that vary rapidly with energy; but when the cross sections are integrated over a Maxwellian distribution, as in almost all astrophysical applications, the effect of the exact positions of the resonances tends to be averaged out. The resulting averaged collision strengths, calculated from Equation (3.19), are given in Tables 3.3 to 3.7, evaluated at  $T = 10,000$  K, a representative nebular temperature. It is convenient to remember that,

**Table 3.3**

Collision strengths  $\Upsilon$  for  $^2S-^2P^o$  transitions in Li-like  $2s$  and Na-like  $3s$  ions

Ion	$2s \ ^2S, 2p \ ^2P^o$	Ion	$3s \ ^2S^o, 3p \ ^2P^o$
C <sup>+3</sup>	8.91	Mg <sup>+</sup>	16.9
N <sup>+4</sup>	6.81	Si <sup>+3</sup>	16.0
O <sup>+5</sup>	5.21		

Cochrane, D. M., & McWhirter, R. W. P. 1983, *PhyS*, 28, 25.  
McWhirter, R. W. P. 1994, *ADNDT*, 57, 39.

Table 3.4

Collision strengths  $\Upsilon$  for  $^2S - ^3P^o$  transitions in Be-like  $2s^2$  and Mg-like  $3s^2$  ions

Ion	$^1S, ^3P^o$	$^3P_0^o, ^3P_1^o$	$^3P_0^o, ^3P_2^o$	$^3P_1^o, ^3P_2^o$
C <sup>+2</sup>	1.05	0.96	0.72	2.78
N <sup>+3</sup>	1.07	1.14	0.83	3.29
O <sup>+4</sup>	0.82	0.67	0.65	2.32
Al <sup>+1</sup>	3.35	1.89	1.94	6.72
Si <sup>+2</sup>	5.56	1.81	3.62	10.4
S <sup>+4</sup>	1.9	—	—	—

C<sup>+2</sup> Berrington, K. A., Burke, P. G., Dufton, P. L., & Kingston, A. E. 1985, ADNDT, 33, 195; N<sup>+3</sup>, O<sup>+4</sup> Ramsbottom, C. A., Berrington, K. A., Hibbert, A., & Bell, K. L. 1994, Physica Scripta, 50, 246; O<sup>+4</sup> McKenna, R. C., et al. 1997, ApJ, 486, 571; Al<sup>+1</sup> Aggarwal, K. M., & Keenan, F. P. 1998, J. Phys B, 31, 4545, and Aggarwal, K. M., & Keenan, F. P. 1994, J. Phys. B, 27, 5321; Si<sup>+2</sup> Dufton, P. L., & Kingston, A. E. 1994, ADNDT, 57, 273; S<sup>+4</sup> Dufton, P. L., & Kingston, A. E. 1984, J. Phys. B, 17, 3321 (extrapolated).

Table 3.5

Collision strengths  $\Upsilon$  for B-like  $2p$ , F-like  $2p^5$ , Al-like  $3p$  and Cl-like  $3p^5$  ions

Ion	$^1P_{1/2}^o, ^1P_{3/2}^o$	Ion	$^1P_{1/2}^o, ^1P_{3/2}^o$
C <sup>+</sup>	2.15	Si <sup>+</sup>	5.70
N <sup>+2</sup>	1.45	S <sup>+3</sup>	8.54
O <sup>+3</sup>	2.34	Ar <sup>+5</sup>	6.33
Ne <sup>+5</sup>	3.21		
Ne <sup>+</sup>	0.28	Ar <sup>+</sup>	2.93
Mg <sup>+3</sup>	0.36	Ca <sup>+3</sup>	1.00
Si <sup>+5</sup>	0.30		

B-like ions from Blum, R. D., & Pradhan, A. K. 1992, ApJS 80, 425; F-like ions from Saraph, H. E. & Tully, J. A. 1994, A&AS, 107, 29; Si<sup>+</sup> Dufton, P. L., & Kingston, A. E. 1994, ADNDT, 57, 273, S<sup>+3</sup> Tayal, S. S. 2000, ApJ, 530, 1091; Ar<sup>+5</sup> Saraph, H. E., & Storey, P. J. 1996, A&AS, 115, 151; Ar<sup>+</sup>, Ca<sup>+3</sup> Pelan, J., & Berrington, K. A. 1995, A&AS, 110, 209.

for an electron with the mean energy at a typical nebular temperature,  $T \approx 7,500$  K, the cross sections for excitation and deexcitation are  $\sigma \approx 10^{-15} \Upsilon / \omega \text{ cm}^2$ .

Note that there is a simple relation for the collision strengths between a term consisting of a single level and a term consisting of various levels, namely,

$$\Upsilon(SLJ, S'L'J') = \frac{(2J' + 1)}{(2S' + 1)(2L' + 1)} \Upsilon(SL, S'L') \quad (3.21)$$

Table 3.6

Collision strengths  $\Upsilon$  for C-like  $2p^2$ , O-like  $2p^4$ , Si-like  $3p^2$  and S-like  $3p^4$  ions

Ion	$^3P, ^1D$	$^3P, ^1S$	$^1D, ^1S$	$^3P_0, ^3P_1$	$^3P_0, ^3P_2$	$^3P_1, ^3P_2$	$^3P, ^5S^o$
N <sup>+</sup>	2.64	0.29	0.83	0.41	0.27	1.12	1.27
O <sup>+2</sup>	2.29	0.29	0.58	0.55	0.27	1.29	0.18
Ne <sup>+4</sup>	2.09	0.25	0.58	1.41	1.81	5.83	1.51
Ne <sup>+2</sup>	1.36	0.15	0.27	0.24	0.21	0.77	—
S <sup>+2</sup>	6.95	1.18	1.38	3.98	1.31	7.87	2.85
Ar <sup>+4</sup>	3.21	0.56	1.65	2.94	1.84	7.81	—
Ar <sup>+2</sup>	4.83	0.84	1.22	1.26	0.67	3.09	—

N<sup>+</sup>, O<sup>+2</sup>, and Ne<sup>+4</sup> from Lennon, D. J., & Burke, V. M. 1994, A&AS, 103, 273; Ne<sup>+2</sup> from Butler, K., & Zeippen, C. J. 1994, A&AS, 108, 1; S<sup>+2</sup> from Tayal, S. S., and Gupta, G. P. 1999 ApJ 526, 544; Ar<sup>+2</sup>, Ar<sup>+4</sup> from Galavis, M. E., Mendoza, C., & Zeippen, C. J. 1995, A&AS, 111, 347.

Table 3.7

Collision strengths  $\Upsilon$  for N-like  $2p^3$  and P-like  $3p^3$  ions

Ion	$^4S^o, ^2D^o$	$^4S^o, ^2P^o$	$^2D_{3/2}^o, ^2D_{5/2}^o$	$^2D_{3/2}^o, ^2P_{1/2}^o$
O <sup>+</sup>	1.34	0.40	1.17	0.28
Ne <sup>+3</sup>	1.40	0.47	1.36	0.34
S <sup>+</sup>	6.90	3.53	7.47	1.79
Ar <sup>+3</sup>	1.90	1.18	7.06	1.51

Ion	$^2D_{3/2}^o, ^2P_{3/2}^o$	$^2D_{5/2}^o, ^2P_{1/2}^o$	$^2D_{3/2}^o, ^2D_{5/2}^o$	$^2P_{1/2}^o, ^2P_{3/2}^o$
O <sup>+</sup>	0.82	0.33	1.23	0.157
Ne <sup>+3</sup>	0.51	0.37	0.90	0.34
S <sup>+</sup>	3.00	2.20	4.99	2.71
Ar <sup>+3</sup>	2.14	1.53	7.06	2.07

O<sup>+</sup> Pradhan, A. K. 1976, MNRAS, 177, 31, 1998, and J Phys B, 31, 4317; Ne<sup>+3</sup>, Giles, K. 1981, MNRAS, 195, 63, and Ramsbottom, C. A., Bell, K. L., & Keenan, F. P. 1998, MNRAS, 293, 233; S<sup>+</sup> Ramsbottom, C. A., Bell, K. L., Stafford, R. P. 1996, ADNDT, 63, 57; Ar<sup>+3</sup> Ramsbottom, C. A., & Bell, K. L. 1997, ADNDT, 66, 65.

if either  $S = 0$  or  $L = 0$ . The factors  $(2J' + 1)$  and  $(2S' + 1)(2L' + 1)$  are the statistical weights of the level and of the term, respectively. On account of this relation, the rate of collisional excitation in  $p^2$  or  $p^4$  ions (such as O<sup>++</sup>) from the ground  $^3P$  term to the excited (singlet)  $^1D$  and  $^1S$  levels is very nearly independent of the distribution of ions among  $^3P_0$ ,  $^3P_1$ , and  $^3P_2$ .

**Table 3.8**  
Transition probabilities for Be-like  $2s^2$  ions

Transition	C III]		N IV]		O V]	
	A (s <sup>-1</sup> )	$\lambda$ (Å)	A (s <sup>-1</sup> )	$\lambda$ (Å)	A (s <sup>-1</sup> )	$\lambda$ (Å)
$^1S_0-^3P_2^o$	0.0052	1906.7	0.011	1483.2	0.022	1213.8
$^1S_0-^3P_1^o$	104	1908.7	0.680	1486.5	2280	1218.3

N IV], Flemming, J., Brage, T., Bell, K. L., Vaeck, N., Hibbert, A., Godefroid, M., & Froese Fischer, C. 1995, *ApJ*, 455, 758; C III], OV], Flemming, J., Bell, K. L. K., Hibbert, A., Vaeck, N., & Godefroid, M. 1996, *MNRAS*, 279, 1289.

**Table 3.9**  
Transition probabilities for B-like  $2p$ , ions

Transition	C II		N III		O IV	
	A (s <sup>-1</sup> )	$\lambda$ (Å)	A (s <sup>-1</sup> )	$\lambda$ (Å)	A (s <sup>-1</sup> )	$\lambda$ (Å)
$^2P_{1/2}^o-^2P_{3/2}^o$	$2.3 \times 10^{-6}$	157.74 $\mu\text{m}$	$4.7 \times 10^{-5}$	57.343 $\mu\text{m}$	$5.2 \times 10^{-4}$	25.913 $\mu\text{m}$
$^2P_{1/2}^o-^4P_{1/2}$	$7.3 \times 10^1$	2324.7	$4.2 \times 10^2$	1748.6	$1.7 \times 10^3$	1399.8
$^2P_{1/2}^o-^4P_{3/2}$	1.6	2323.6	$1.2 \times 10^2$	1746.8	$4.8 \times 10^1$	1397.2
$^2P_{3/2}^o-^4P_{1/2}$	$7.6 \times 10^1$	2328.1	4.5	1754.0	$1.8 \times 10^3$	1407.4
$^2P_{3/2}^o-^4P_{3/2}$	$1.1 \times 10^1$	2326.9	$7.0 \times 10^1$	1752.2	$3.1 \times 10^2$	1404.8
$^2P_{3/2}^o-^4P_{5/2}$	$5.3 \times 10^1$	2325.4	$3.2 \times 10^2$	1749.7	$1.3 \times 10^3$	1401.2

Galavis, M. E., Mendoza, C., & Zeppen, C. J. 1998, *A&AS*, 131, 499; Wiese, W. L., Fuhr, J. R., & Deters, T. M. 1996, *J. Chem Phys Ref Data Monograph No. 7*; Kaufman, J., & Sugar, J. 1986, *J. Chem Phys Ref Data* 15, 321.

For all the low-lying levels of the ions listed in Tables 3.3 through 3.5, the excited levels arise from the same electron configurations as the ground level. Radiative transitions between these excited levels and the ground level are forbidden by the electric-dipole selection rules, but can occur by magnetic-dipole and/or electric-quadrupole transitions. These are the well known forbidden lines, many of which are observed in nebular spectra, in the optical, infrared, or ultraviolet regions. Transition probabilities, as well as wavelengths for the observable lines, are listed in Tables 3.8 through 3.14.

For an ion with a single excited level, in the limit of very low electron density, every collisional excitation is followed by the emission of a photon, and the cooling rate per unit volume is therefore

$$L_C = n_e n_1 q_{12} h\nu_{21}. \quad (3.22)$$

**Table 3.10**  
Transition probabilities for Al-like 3*p* ions

Transition	Si II		S IV	
	A (s <sup>-1</sup> )	λ (Å)	A (s <sup>-1</sup> )	λ (Å)
<sup>2</sup> P <sub>1/2</sub> <sup>o</sup> - <sup>2</sup> P <sub>3/2</sub> <sup>o</sup>	2.2 × 10 <sup>-4</sup>	34.814 μm	7.8 × 10 <sup>-3</sup>	10.514 μm
<sup>2</sup> P <sub>1/2</sub> <sup>o</sup> - <sup>4</sup> P <sub>1/2</sub>	6.3 × 10 <sup>3</sup>	2334.4	5.1 × 10 <sup>4</sup>	1408.8
<sup>2</sup> P <sub>1/2</sub> <sup>o</sup> - <sup>4</sup> P <sub>3/2</sub>	2.0 × 10 <sup>1</sup>	2328.5	7.0 × 10 <sup>2</sup>	1395.1
<sup>2</sup> P <sub>3/2</sub> <sup>o</sup> - <sup>4</sup> P <sub>1/2</sub>	4.9 × 10 <sup>3</sup>	2350.2	3.8 × 10 <sup>4</sup>	1420.5
<sup>2</sup> P <sub>3/2</sub> <sup>o</sup> - <sup>4</sup> P <sub>3/2</sub>	1.7 × 10 <sup>3</sup>	2344.2	1.5 × 10 <sup>4</sup>	1413.6
<sup>2</sup> P <sub>3/2</sub> <sup>o</sup> - <sup>4</sup> P <sub>5/2</sub>	2.7 × 10 <sup>3</sup>	2334.6	3.5 × 10 <sup>4</sup>	1402.8

Si II, Dufton, P. L., & Kingston, A. E. 1991, MNRAS, 248, 827; S IV; λ and A(UV), Gupta, G. P., & Msezane, A. Z. 2000, ApJS, 130, 227; S<sup>4+</sup> A(IR), Johnson, C. T., Kingston, A. E., Dufton, P. L. 1986, MNRAS 220, 155.

**Table 3.11**  
Transition probabilities for <sup>2</sup>P<sub>3/2</sub><sup>o</sup> - <sup>2</sup>P<sub>1/2</sub><sup>o</sup> in F-like 2*p*<sup>5</sup> and Cl-like 3*p*<sup>5</sup> ions

Ion	A (s <sup>-1</sup> )	λ (μm)
Ne II	8.6 × 10 <sup>-3</sup>	12.814
Mg IV	2.0 × 10 <sup>-1</sup>	4.487
Ar II	5.3 × 10 <sup>-2</sup>	6.983
Ca IV	5.5 × 10 <sup>-1</sup>	3.206

Kaufman, J., & Sugar, J. 1986, J. Chem. Phys. Ref. Data 15, 321.

However, if the density is sufficiently high, collisional deexcitation is not negligible and the cooling efficiency is reduced. The equilibrium equation for the balance between the excitation and deexcitation rates of the excited level is, in general,

$$n_e n_1 q_{12} = n_e n_2 q_{21} + n_2 A_{21}, \quad (3.23)$$

and the solution is

$$\frac{n_2}{n_1} = \frac{n_e q_{12}}{A_{21}} \left[ \frac{1}{1 + \frac{n_e q_{21}}{A_{21}}} \right], \quad (3.24)$$

(3.22)

Table 3.12

Transition probabilities for C-like  $2p^2$  and Si-like  $3p^2$  ions

Transition	[N II]		[O III]		[Ne V]		[S III]		[Ar V]	
	$A$ ( $s^{-1}$ )	$\lambda$ ( $\text{\AA}$ )	$A$ ( $s^{-1}$ )	$\lambda$ ( $\text{\AA}$ )	$A$ ( $s^{-1}$ )	$\lambda$ ( $\text{\AA}$ )	$A$ ( $s^{-1}$ )	$\lambda$ ( $\text{\AA}$ )	$A$ ( $s^{-1}$ )	$\lambda$ ( $\text{\AA}$ )
$^1D_2-^1S_0$	1.0	5754.6	1.6	4363.2	2.8	2972.8	2.3	6312.0	3.5	4625.3
$^3P_2-^1S_0$	$1.3 \times 10^{-4}$	3070.8	$6.1 \times 10^{-4}$	2331.4	$6.3 \times 10^{-3}$	1593.3	$1.3 \times 10^{-2}$	3797.2	$6.8 \times 10^{-2}$	2786.0
$^3P_1-^1S_0$	$3.3 \times 10^{-2}$	3062.8	$2.3 \times 10^{-1}$	2321.0	4.0	1574.6	$8.4 \times 10^{-1}$	3721.7	6.7	2691.0
$^3P_2-^1D_2$	$3.0 \times 10^{-3}$	6583.4	$2.0 \times 10^{-2}$	5006.9	$3.5 \times 10^{-1}$	3425.9	$5.5 \times 10^{-2}$	9531.0	$4.7 \times 10^{-1}$	7005.9
$^3P_1-^1D_2$	$9.8 \times 10^{-4}$	6548.0	$6.8 \times 10^{-3}$	4958.9	$1.2 \times 10^{-1}$	3345.9	$2.1 \times 10^{-2}$	9068.9	$2.0 \times 10^{-1}$	6435.1
$^3P_0-^1D_2$	$3.6 \times 10^{-7}$	6527.1	$1.7 \times 10^{-6}$	4931.1	$1.9 \times 10^{-5}$	3300.5	$1.3 \times 10^{-5}$	8829.9	$6.1 \times 10^{-5}$	6133.8
$^3P_1-^3P_2$	$7.5 \times 10^{-6}$	121.89 $\mu\text{m}$	$9.7 \times 10^{-5}$	51.814 $\mu\text{m}$	$4.6 \times 10^{-3}$	14.32 $\mu\text{m}$	$2.1 \times 10^{-3}$	18.713 $\mu\text{m}$	$2.7 \times 10^{-2}$	7.9 $\mu\text{m}$
$^3P_0-^3P_2$	$1.1 \times 10^{-12}$	76.5 $\mu\text{m}$	$3.1 \times 10^{-11}$	32.661 $\mu\text{m}$	$5.0 \times 10^{-9}$	9.01 $\mu\text{m}$	$4.3 \times 10^{-8}$	12.00 $\mu\text{m}$	$1.2 \times 10^{-6}$	4.9 $\mu\text{m}$
$^3P_0-^3P_1$	$2.1 \times 10^{-6}$	205.5 $\mu\text{m}$	$2.7 \times 10^{-5}$	88.356 $\mu\text{m}$	$1.3 \times 10^{-3}$	24.28 $\mu\text{m}$	$4.7 \times 10^{-4}$	33.47 $\mu\text{m}$	$8.0 \times 10^{-3}$	13.1 $\mu\text{m}$
$^3P_2-^5S_2^o$	$1.3 \times 10^{+2}$	2142.8	$5.8 \times 10^{+2}$	1666.2	$6.0 \times 10^{+3}$	1146.1	$1.2 \times 10^4$	1728.9	—	—
$^3P_1-^5S_2^o$	$5.5 \times 10^{+1}$	2139.0	$2.4 \times 10^{+2}$	1660.8	$2.4 \times 10^3$	1137.0	$4.4 \times 10^3$	1713.1	—	—

C-like: Galavis, M. E., Mendoza, C., & Zeppen, C. J. 1997, A&AS, 123, 159; Mendoza, C., Zeppen, C. J., & Storey, P. J. 1999, A&AS, 135, 159; Storey, P. J. & Zeppen, C. J. 2000, MNRAS, 312, 813; Si-like: Tayal, S. S. 1997, ADNDT, 67, 331; Biemont, E., & Bromage, G. E. 1983, MNRAS, 205, 1085.

Table 3.13

Transition probabilities of N-like  $2p^3$  and P-like  $3p^3$  ions

Transition	[N I]		[O II]		[Ne IV]		[S II]		[Ar IV]	
	$A$ ( $s^{-1}$ )	$\lambda$ ( $\text{\AA}$ )	$A$ ( $s^{-1}$ )	$\lambda$ ( $\text{\AA}$ )	$A$ ( $s^{-1}$ )	$\lambda$ ( $\text{\AA}$ )	$A$ ( $s^{-1}$ )	$\lambda$ ( $\text{\AA}$ )	$A$ ( $s^{-1}$ )	$\lambda$ ( $\text{\AA}$ )
$^2P_{1/2}^o - ^2P_{3/2}^o$	$5.1 \times 10^{-13}$	$25.9 \mu\text{m}$	$1.3 \times 10^{-10}$	$5.01 \mu\text{m}$	$2.6 \times 10^{-9}$	$1.56 \mu\text{m}$	$1.0 \times 10^{-6}$	$214.10 \mu\text{m}$	$4.9 \times 10^{-5}$	$56.47 \mu\text{m}$
$^2D_{5/2}^o - ^2P_{3/2}^o$	$6.1 \times 10^{-2}$	10397.7	$1.1 \times 10^{-1}$	7319.9	$3.9 \times 10^{-1}$	4714.2	$1.8 \times 10^{-1}$	10320.4	$6.0 \times 10^{-1}$	7237.5
$^2D_{3/2}^o - ^2P_{3/2}^o$	$2.8 \times 10^{-2}$	10407.2	$5.8 \times 10^{-2}$	7330.7	$4.3 \times 10^{-1}$	4724.2	$1.3 \times 10^{-1}$	10286.7	$7.9 \times 10^{-1}$	7170.5
$^2D_{5/2}^o - ^2P_{1/2}^o$	$3.5 \times 10^{-2}$	10398.1	$5.6 \times 10^{-2}$	7318.8	$1.1 \times 10^{-1}$	4715.6	$7.8 \times 10^{-2}$	10370.5	$1.2 \times 10^{-1}$	7331.4
$^2D_{3/2}^o - ^2P_{1/2}^o$	$5.3 \times 10^{-2}$	10407.6	$9.4 \times 10^{-2}$	7329.6	$3.8 \times 10^{-1}$	4725.6	$1.6 \times 10^{-1}$	10336.3	$6.0 \times 10^{-1}$	7262.7
$^4S_{3/2}^o - ^2P_{3/2}^o$	$6.6 \times 10^{-3}$	3466.5	$5.7 \times 10^{-2}$	2470.3	$1.2 \times 10^0$	1600.0	$2.2 \times 10^{-1}$	4068.6	2.6	2853.7
$^4S_{3/2}^o - ^2P_{1/2}^o$	$2.7 \times 10^{-3}$	3466.5	$2.3 \times 10^{-2}$	2470.2	$5.0 \times 10^{-1}$	1600.1	$9.1 \times 10^{-2}$	4076.4	$8.6 \times 10^{-1}$	2868.2
$^2D_{5/2}^o - ^2D_{3/2}^o$	$1.1 \times 10^{-8}$	$1.148 \mu\text{m}$	$1.3 \times 10^{-7}$	$497.1 \mu\text{m}$	$1.5 \times 10^{-6}$	$223.7 \mu\text{m}$	$3.3 \times 10^{-7}$	$314.5 \mu\text{m}$	$2.3 \times 10^{-5}$	$77.41 \mu\text{m}$
$^4S_{3/2}^o - ^2D_{5/2}^o$	$6.9 \times 10^{-6}$	5200.3	$3.6 \times 10^{-5}$	3728.8	$4.4 \times 10^{-4}$	2420.9	$2.6 \times 10^{-4}$	6716.5	$1.8 \times 10^{-3}$	4711.3
$^4S_{3/2}^o - ^2D_{3/2}^o$	$1.6 \times 10^{-5}$	5197.9	$1.8 \times 10^{-4}$	3726.0	$5.5 \times 10^{-3}$	2418.2	$8.8 \times 10^{-4}$	6730.8	$2.2 \times 10^{-2}$	4740.2

[O II] Zeippen, C. J. 1987, A&A, 173, 410; [Ne IV] Becker, S. R., Butler, K., & Zeippen, C. J. 1989, A&A, 221, 375; P-like from Menzoda, C., & Zeippen, C. J. 1982, MNRAS, 198, 127; [N I] wavelengths from Slanger, T. G., Huestis, D. L., Cosby, P. C., Osterbrock, D. E. 2000, J. Chem. Phys. 113, 8514.

**Table 3.14**  
Transition probabilities of O-like  $2p^4$  and S-like  $3p^4$  ions

Transition	[O I]		[Ne III]		[Ar III]	
	$A$ ( $s^{-1}$ )	$\lambda$ ( $\text{\AA}$ )	$A$ ( $s^{-1}$ )	$\lambda$ ( $\text{\AA}$ )	$A$ ( $s^{-1}$ )	$\lambda$ ( $\text{\AA}$ )
$^1D_2-^1S_0$	1.1	5577.3	$2.6 \times 10^0$	3342.4	$2.6 \times 10^0$	5191.8
$^3P_2-^1S_0$	$2.9 \times 10^{-4}$	2958.4	$4.0 \times 10^{-3}$	1793.7	$4.2 \times 10^{-2}$	3005.4
$^3P_1-^1S_0$	$7.9 \times 10^{-2}$	2972.3	$2.0 \times 10^0$	1814.6	$3.9 \times 10^0$	3109.2
$^3P_2-^1D_2$	$6.4 \times 10^{-3}$	6300.3	$1.7 \times 10^{-1}$	3868.8	$3.1 \times 10^{-1}$	7135.8
$^3P_1-^1D_2$	$2.1 \times 10^{-3}$	6363.8	$5.4 \times 10^{-2}$	3967.5	$8.2 \times 10^{-2}$	7751.1
$^3P_0-^1D_2$	$6.4 \times 10^{-7}$	6391.8	$8.3 \times 10^{-6}$	4011.7	$2.2 \times 10^{-5}$	8036.9
$^3P_1-^3P_0$	$1.8 \times 10^{-5}$	145.53 $\mu\text{m}$	$1.2 \times 10^{-3}$	36.02 $\mu\text{m}$	$5.2 \times 10^{-3}$	21.842 $\mu\text{m}$
$^3P_2-^3P_0$	$1.3 \times 10^{-10}$	44.047 $\mu\text{m}$	$2.1 \times 10^{-8}$	10.86 $\mu\text{m}$	$2.4 \times 10^{-6}$	6.3692 $\mu\text{m}$
$^3P_2-^3P_1$	$8.9 \times 10^{-5}$	63.184 $\mu\text{m}$	$6.0 \times 10^{-3}$	15.555 $\mu\text{m}$	$3.1 \times 10^{-2}$	8.9910 $\mu\text{m}$

[O I], [Ne III] Galavis, M. E., Mendoza, C., & Zeippen, C. J. 1997, *A&AS*, 123, 159; Storey, P. J., & Zeippen, C. J. 2000, *MNRAS*, 312, 813; [Ar III] Mendoza, C., & Zeippen, C. J. 1983, *MNRAS*, 202, 981.

so the cooling rate is

$$L_C = n_2 A_{21} h\nu_{21} = n_e n_1 q_{12} h\nu_{21} \left[ \frac{1}{1 + \frac{n_e q_{21}}{A_{21}}} \right] \quad (3.25)$$

It can be seen that as  $n_e \rightarrow 0$ , we recover Equation (3.22), but as  $n_e \rightarrow \infty$ ,

$$L_C \rightarrow n_1 \frac{\omega_2}{\omega_1} \exp(-\chi/kT) A_{21} h\nu_{21}, \quad (3.26)$$

the thermodynamic-equilibrium cooling rate.

Some ions have only two low-lying levels and may be treated by this simple formalism, but most ions have more levels, and all ions with ground configurations  $p^2$ ,  $p^3$ , or  $p^4$  have five low-lying levels. Examples are  $O^{++}$  and  $N^+$ , whose energy-level diagrams are shown in Figure 3.1. For such ions, collisional and radiative transitions can occur between any of the levels, and excitation and deexcitation cross sections and collision strengths exist between all pairs of the levels.

The equilibrium equations for each of the levels  $i = 1, 5$  thus become

$$\sum_{j \neq i} n_j n_e q_{ji} + \sum_{j > i} n_j A_{ji} = \sum_{j \neq i} n_i n_e q_{ij} + \sum_{j < i} n_i A_{ij} \quad (3.27)$$

which, together with the total number of ions

$$\sum_j n_j = n, \quad (3.28)$$

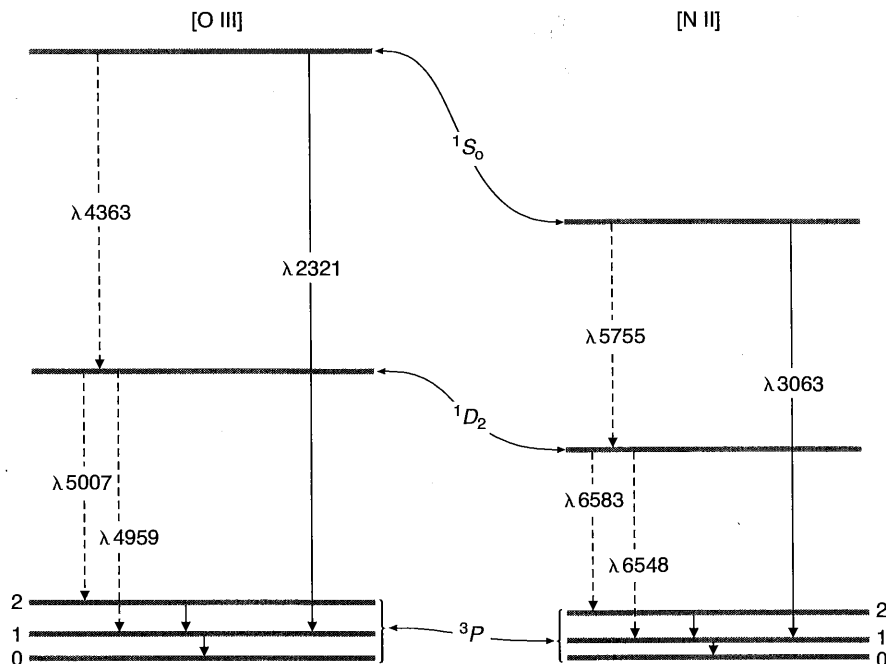


**Figure 3.1**  
 Energy-level diagram for lowest terms of [O III], all from ground  $2p^2$  configuration, and for [N II] of the same isoelectronic sequence. Splitting of the ground  $3P$  term has been exaggerated for clarity. Emission lines in the optical region are indicated by dashed lines, and by solid lines in the infrared and ultraviolet. Only the strongest transitions are indicated.

can be solved for the relative population in each level, and then for the collisionally excited radiative cooling rate

$$L_C = \sum_i n_i \sum_{j < i} A_{ij} h\nu_{ij} \text{ [erg cm}^{-3} \text{ s}^{-1}\text{]}. \quad (3.29)$$

In the low-density limit,  $n_e \rightarrow 0$ , this becomes a sum of terms like (3.22), but if

$$n_e q_{ij} > \sum_{k < i} A_{ik}$$

for any  $i, j$ , collisional deexcitation is not negligible and the complete solution must be used. In fact, for any level  $i$ , a critical density  $n_c(i)$  may be defined as

$$n_c(i) = \sum_{j < i} A_{ij} / \sum_{j \neq i} q_{ij} \quad (3.30)$$

**Table 3.15**  
Critical densities for collisional deexcitation

Ion	Level	$n_e$ (cm <sup>-3</sup> )	Ion	Level	$n_e$ (cm <sup>-3</sup> )
C II	$2P_{3/2}^o$	$5.0 \times 10^1$	O III	$1D_2$	$6.8 \times 10^5$
C III	$3P_2^o$	$5.1 \times 10^5$	O III	$3P_2$	$3.6 \times 10^3$
N II	$1D_2$	$6.6 \times 10^4$	O III	$3P_1$	$5.1 \times 10^2$
N II	$3P_2$	$3.1 \times 10^2$	Ne II	$2P_{1/2}^o$	$7.1 \times 10^5$
N II	$3P_1$	$8.0 \times 10^1$	Ne III	$1D_2$	$9.5 \times 10^6$
N III	$2P_{3/2}^o$	$1.5 \times 10^3$	Ne III	$3P_0$	$3.1 \times 10^4$
N IV	$3P_2^o$	$1.1 \times 10^6$	Ne III	$3P_1$	$2.1 \times 10^5$
O II	$2D_{3/2}^o$	$1.5 \times 10^4$	Ne V	$1D_2$	$1.3 \times 10^7$
O II	$2D_{5/2}^o$	$3.4 \times 10^3$	Ne V	$3P_2$	$3.5 \times 10^4$
S II	$2D_{3/2}^o$	$5.4 \times 10^4$	Ne V	$3P_1$	$6.2 \times 10^3$
S II	$2D_{5/2}^o$	$1.6 \times 10^4$			

NOTE: All values are calculated for  $T = 10,000$  K.

so that for  $n_e < n_c(i)$ , collisional deexcitation of level  $i$  is negligible, but for  $n_e > n_c(i)$  it is important. Critical densities for levels that are most important in radiative cooling are listed in Table 3.15.

### 3.6 Energy Loss by Collisionally Excited Line Radiation of H

$H^+$ , the most abundant ion in nebulae, has no bound levels and no lines, but  $H^0$ , although its fractional abundance is low, may affect the radiative cooling in a nebula. The most important excitation processes from the ground  $1^2S$  term are to  $2^2P^o$ , followed by emission of a  $L\alpha$  photon with  $h\nu = 10.2$  eV, and to  $2^2S$ , followed by emission of two photons in the  $2^2S \rightarrow 1^2S$  continuum with  $h\nu' + h\nu'' = 10.2$  eV and transition probability  $A(2^2S, 1^2S) = 8.23 \text{ s}^{-1}$ . Cross sections for excitation of neutral atoms by electrons do not vary as  $u^{-2}$ , but rise from zero at the threshold, peak at energies several times the threshold, and then decline at high energies, often with superimposed resonances. Nevertheless the mean collision strengths, integrated over the Maxwellian velocity distribution of the electrons as defined by (3.18) and (3.19), for these transitions and for  $1^2S \rightarrow 3^2S$ ,  $3^2P^o$ , and  $3^2D$  are quantities that vary fairly slowly, as Table 3.16 shows.

### 3.7 Resulting Thermal Equilibrium

The temperature at each point in a static nebula is determined by the equilibrium between heating and cooling rates, namely,

$$G = L_R + L_{FF} + L_C. \quad (3.31)$$

**Table 3.16**  
Effective collision strengths for H I

$T(K)$	$1^2S, 2^2S$	$1^2S, 2^2P^o$	$1^2S, 3^2S$	$1^2S, 3^2P^o$	$1^2S, 3^2D$
10,000	0.29	0.51	0.066	0.12	0.063
15,000	0.32	0.60	0.071	0.13	0.068
20,000	0.35	0.69	0.077	0.14	0.073

Anderson, H., Balance, C. P., Badnell, N. R., & Summers, H. P. 2000, J.Phys.B, 33, 1255.

The collisionally excited radiative cooling rate  $L_C$  is a sum (over all transitions of all ions) of individual terms like (3.22), (3.25), or (3.29). In the low-density limit, since all the terms in  $G$ ,  $L_R$ ,  $L_{FF}$ , and  $L_C$  are proportional to  $n_e$  and to the density of some ion, Equation (3.31) and therefore the resulting temperatures are independent of the total density, but do depend on the relative abundances of the various ions. When collisional deexcitation begins to be important, the cooling rate at a given temperature is decreased, and the equilibrium temperature for a given radiation field is therefore somewhat increased.

To understand better the concepts here, let us consider an example, namely, an H II region with “typical” abundances of the elements. We will adopt  $n(O)/n(H) = 7 \times 10^{-4}$ ,  $n(Ne)/n(H) = 9 \times 10^{-5}$ , and  $n(N)/n(H) = 9 \times 10^{-5}$ , and neglect other elements for simplicity. Let us suppose that O, Ne, and N are each 80 percent singly ionized and 20 percent doubly ionized, and  $n(H^0)/n(H) = 1 \times 10^{-3}$ . Some of the individual contributions to the radiative cooling (in the low-density limit) and the total radiative cooling  $L_C + L_{FF}$  are shown in Figure 3.2. For each level the contribution is small if  $kT \ll \chi$ , then increases rapidly and peaks at  $kT \approx \chi$ , and then decreases slowly for  $kT > \chi$ . The total radiative cooling, composed of the sum of the individual contributions, continues to rise with increasing  $T$  as long as there are levels with excitation energy  $\chi > kT$ . It can be seen that, for the assumed composition and ionization,  $O^{++}$  dominates the radiative cooling contribution at low temperatures, and  $O^+$  at somewhat higher temperatures. At all temperatures shown, the contribution of collisional excitation of  $H^0$  is small.

It is convenient to rewrite Equation (3.31) in the form

$$G - L_R = L_{FF} + L_C,$$

where  $G - L_R$  is then the “effective heating rate”, representing the net energy gained in photoionization processes, with the recombination losses already subtracted. This effective heating rate is also shown in Figure 3.2, for model stellar atmospheres with various temperatures. Notice in the figure that the calculated nebular temperature at which the curves cross and at which Equation (3.31) is satisfied is rather insensitive to the input stellar radiation field. Typical nebular temperatures are  $T \approx 7,000$  K, according to Figure 3.2, with somewhat higher temperatures for hotter stars or larger optical depths.

( $\text{cm}^{-3}$ )

$8 \times 10^5$

$6 \times 10^3$

$1 \times 10^2$

$1 \times 10^5$

$5 \times 10^6$

$1 \times 10^4$

$1 \times 10^5$

$3 \times 10^7$

$5 \times 10^4$

$2 \times 10^3$

$> n_c(i)$

cooling

out  $H^0$ ,

nebula.

$2^2P^o$ ,

wed by

0.2 eV

tion of

eshold,

s, often

egrated

8) and

ies that

ilibrium

(3.31)

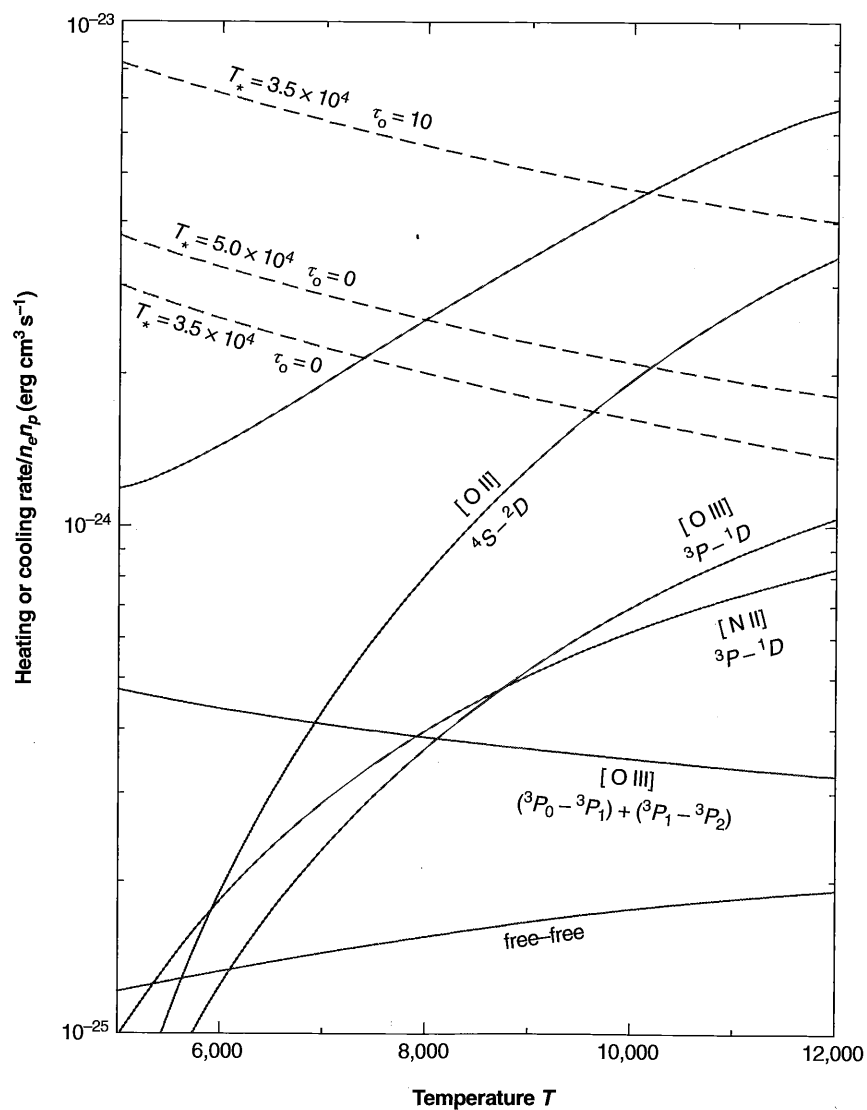


Figure 3.2

Net effective heating rates ( $G - L_R$ ) for various stellar input spectra, shown as dashed curves. Total radiative cooling rate ( $L_{FF} + L_C$ ) for the simple approximation to the H II region described in the text is shown as highest solid black curve, and the most important individual contributions to radiative cooling are shown by labeled solid curves. The equilibrium temperature is given by the intersection of a dashed curve and the highest solid curve. Note how the increased optical depth,  $\tau_0$ , or increased stellar temperature,  $T_*$ , increases  $T$  by increasing  $G$ .

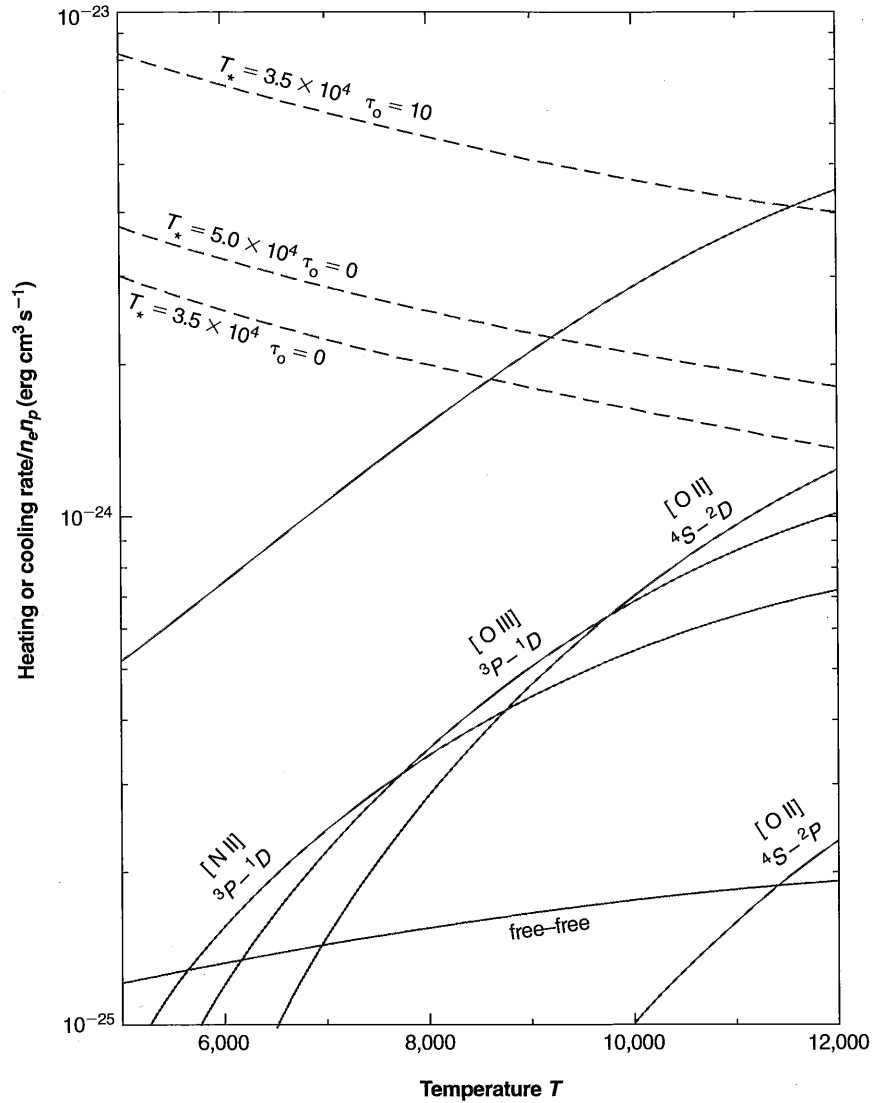


Figure 3.3

Same as Figure 3.2, except that collisional deexcitation at  $n_e = 10^4 \text{ cm}^{-3}$  has been approximately taken into account in the radiative cooling rates.

ashed  
e H II  
portant  
ilibrium  
e. Note  
T by

At high electron densities, collisional deexcitation can appreciably modify the radiative cooling rate and therefore the resulting nebular temperature. For instance, at  $n_e \approx 10^4 \text{ cm}^{-3}$ , a density that occurs in condensations in many H II regions, the [O II]  $^4S-^2D$  and [O III]  $^3P_0-^3P_1$  and  $^3P_0-^3P_2$  transitions are only about 20 percent effective, [N II]  $^3P_0-^3P_1$  and  $^3P_0-^3P_2$  are only about 1 percent effective, and [N III]  $^2P_{1/2}-^2P_{3/2}$  is about 20 percent effective, as Table 3.15 shows. Figure 3.3 shows the effective cooling rate for this situation, with the abundances and ionization otherwise as previously described, and demonstrates that appreciably higher temperatures occur at high densities. Similarly, lower abundances of the heavy elements tend to decrease the cooling rate and thus to increase the resulting equilibrium temperature.

Under conditions of very high ionization, however, as in the central part of a planetary nebula, the ionization is high enough that there is very little  $\text{H}^0$ ,  $\text{O}^+$ , or  $\text{O}^{++}$ , and then the radiative cooling is appreciably decreased. Under these conditions the main coolants are  $\text{Ne}^{+4}$  and  $\text{C}^{+3}$ , and the nebular temperature may be  $T \lesssim 2 \times 10^4 \text{ K}$ . Detailed results obtained from models of both H II regions and planetary nebulae are discussed in Chapter 5.

## References

The basic papers on thermal equilibrium are:

- Spitzer, L. 1948, ApJ, 107, 6.
- Spitzer, L. 1949, ApJ, 109, 337.
- Spitzer, L., & Savedoff, M. P. 1950, Ap. J. 111, 593.

Some additional work, including the on-the-spot approximation and the effects of collisional deexcitation, is described in

- Burbidge, G. R., Gould, R. J., and Pottasch, S. R. 1963, ApJ, 138, 945.
- Osterbrock, D. E. 1965, ApJ, 142, 1423.

Numerical values of recombination coefficients,  $\beta$ , are given in

- Hummer, D. G., & Seaton, M. J. 1963, MNRAS, 125, 437.
- Seaton, M. J. 1959, MNRAS, 119, 81.
- Ferland, G. J., Peterson, B. M., Horne, K., Welsh, W. F., & Nahar, S. 1992, ApJ, 387, 95.
- Hummer, D. G. 1994, MNRAS, 268, 109.
- LaMothe, J., & Ferland, G. J. 2001, PASP, 113, 165.

(Table 3.2 is based on these references.)

Extensive tables of the free-free Gaunt factor are given by

- Karzas, W. J., & Latter, R. 1961, ApJS, 6, 167.
- Carson, T. R. 1988, A&A, 189, 319.
- Kylafis, N. D., & Lamb, D. Q. 1982, ApJS, 48, 239.

Basic papers on collisional excitation and the methods used to calculate the collision strengths are:

Seaton, M. J. 1968, *Advances in Atomic and Molecular Physics* 4, 331.

Seaton, M. J. 1975, *Advances in Atomic and Molecular Physics* 11, 83.

This material is further elucidated in the book

Burke, P. G., Eissner, W. B., Hummer, D. G., & Percival, I. C., eds. 1983, *Atoms in Astrophysics* (New York: Plenum Press).

Numerical values of collision strengths are widely scattered through the physics literature, but mostly in the journals *Atomic Data Nuclear Data Tables* (ADNDT), *Journal of Physics B* (J. Phys. B), *Physics Review A* (Phys Rev A), and *Physica Scripta* (PhySc). Volume 57 of ADNDT consists of a number of reviews of sources for collision strengths.

Today many data bases are located on the web. Among others, check the

Chianti: <http://www.solar.nrl.navy.mil/chianti.html>

TopBase, the Opacity Project database <http://heasarc.gsfc.nasa.gov/topbase/>

ADfA database <http://www.pa.uky.edu/~verner/atom.html>

The best wavelengths come from nebular measurements made with high-dispersion spectrographs. The following give extensive emission line lists.

Kaufman, V., & Sugar, J. 1986, *J. Phys. Chem. Ref. Data*, 15, No. 1, 321 (forbidden lines).

House, L.L. 1969, *ApJS*, 155, 21 (X-ray).

Hyung, S., & Aller, L. H. 1997, *ApJ*, 491, 242 (ultraviolet and optical).

Feuchtgruber, H., Lutz, D., et al., 1997, *ApJ*, 487, 962 and Feuchtgruber, H., Lutz, D., & Beintema, D. A., 2001, *ApJS*, 136, 221 (infrared).

<http://www.pa.uky.edu/~peter/atomic/> is a web-based list of wavelengths.

The following is the most recent in a series of papers that give a bibliography of atomic line identifications:

Adelman, S. J. 2001, *PASP*, 113, 344.